Interreg CENTRAL EUROPE

Co-funded by the European Union

MAURICE

D2.3.3

Effects of climate change on agricultural practice, irrigation and groundwater levels - Report

Version 2

06 2026

Interreg CENTRAL EUROPE

Co-funded by the European Union

MAURICE

D2.3.3

Effects of climate change on agricultural practice, irrigation and groundwater levels – Report

Contributors

Paolo Colombo[1]

Rachele Riva[2]

Enrico Weber[3]

Claudio Gandolfi[2]

Luca Alberti[1]

[1]Department of Civil and Environmental Engineering, Politecnico di Milano, Milan, Italy

[2]Department of Agricultural and Environmental Sciences - Production, Territory, Agroenergy, Università degli Studi di Milano, Milan, Italy

[3]Softwater S.r.l., Milan, Italy

Table of contents

A. Introduction

Climate and adaptation scenarios have been simulated via the agro-hydrological and hydrogeological models described in Deliverable 2.3.2 for the MAURICE Pilot Action set in Milan. The measure tested in the Pilot Action is an Agricultural-Managed Aquifer Recharge solution involving the distribution of water along canals and over agricultural fields during winter via the most common irrigation practice in the study area (located in the Po plain in the Consorzio Est Ticino Villoresi territory), the surface/furrows irrigation method. This method enables the percolation of high percentages of the mobilized water coming from surface water bodies, thus representing an additional inflow towards the aquifer system. The application of the measure in periods of water availability can serve as a drought preparedness measure, storing additional volumes of water that can be later extracted to sustain a dry period, as well as a drought recovery measure, helping the aquifer recover after a drought.

Different scenarios have been simulated and analysed (described in Section 2.2). Simulations via modelling tools are the standard practice to assess measures in adapting to climate change. How the measure is assessed depends on indicators chosen. After analysing the differences between the percolations observed and the projections (Section 1), this report analyses the results of simulations in terms of the volume able to be stored in the aquifer and on the groundwater dependent ecosystems that get influenced (Section 4.1). The analysis concentrated then on the influence of the infiltration areas distribution as well as the performance in extremely dry periods (Sections 4.2 and 4.3).

The results are also made available to be interactively explored in a dashboard deployed for the project, available at: maurice.soft-water.it. The description of the dashboard content is provided in Deliverable 2.4.1. The goal of the dashboard is for it to be accessible to policymakers and stakeholders to make them understand the opportunities of the measure and ease the implementation in their plans.

Overall, the measure can be an ally in adapting to climate change. It needs a sound governance system to determine the implementation strategy, field distribution, and the balance between the two main objectives: volume stored and lowland springs maintenance. The management of the emergency extractions is also a crucial aspect to be considered, to avoid extra stresses to the aquifer and overconsumption. The Pilot Action can be considered successful in its main goal of testing this simple but impactful measure and rendering it a potential adaptation tool for irrigation consortia and water managers. The guidelines on its implementation and lessons learned from the Pilot Action are reported in Deliverable 2.4.2.

B. Water balance under climate change scenarios

1. Analysis of percolation under CC

The application of the sub-district level implementation of the IdrAgra model, as described in Deliverable 2.3.2, has made it possible to simulate the period 2019–2050 using projections of climatic conditions and of discharge values in the Villoresi Canal as input data. Three different sets of climate projections were considered, each derived from the results of a different regional circulation model (RCM), namely: CNRM-ALADIN63, KNMI-RACMO22E and ICTP-RegCM4-6, hereafter referred to as Aladin, RACMO and RegCM4, respectively. The estimation of climate and Villoresi Canal discharge projections is detailed in Deliverable 2.4.1.

For the 2019-2025 control period, the RCM-driven simulations were compared against the corresponding simulation obtained using historical meteorological data and observed values of canal discharge. This comparison was carried out to assess how well the RCM-driven simulations reproduce the magnitude and temporal dynamics of percolation over the historical reference period.

Figure 1 shows the annual cumulative percolation volume obtained with historical forcing and with the three RCM-driven simulations. For the years 2023–2025, the cumulative volumes also include the contribution associated with winter irrigation. The dashed horizontal line indicates the median annual percolation volume of the Historical series over the 2019–2025 control period.

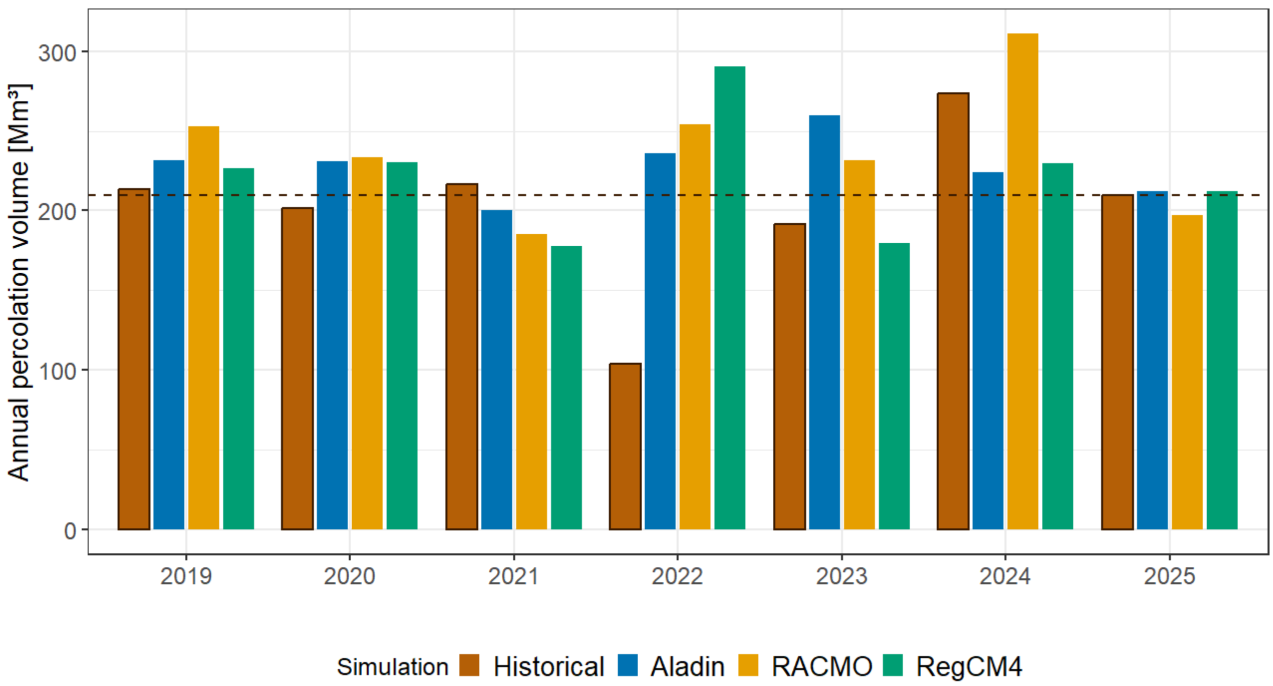

Figure 1. Annual percolation volume [Mm^3] of the Pilot Area estimated with historical meteorological data and observed canal discharges and with meteorological data and Villoresi Canal discharges projected using the RCMs Aladin, RACMO and RegCM4.

The 2022-2023 period was characterized by a severe hydrological drought in northern Italy, which ended only after the rainfall events of May 2023. None of the RCM-driven simulations reproduced conditions as extreme as those observed in 2022. The annual percolation volume obtained with historical forcing in 2022 is markedly lower than the 2019–2025 Historical median, whereas the RCM-driven simulations remain closer to the average behaviour of the control period.

The monthly time series (Figure 2) provide a more detailed view of the temporal agreement between the RCM-driven simulations and the Historical reference. Overall, the three RCMs reproduce the main seasonal pattern of percolation and capture most of the monthly peaks. However, they strongly diverge from the Historical series during 2022, when the historical simulation shows a marked reduction in percolation that is not reproduced by any of the RCM-driven simulations. The comparison also shows that the differences are seasonally structured. During the summer irrigation period, absolute differences are generally more relevant because monthly percolation volumes are higher. During the winter season, relative deviations tend to be higher, as the Historical reference volumes are lower and even moderate absolute differences translate into larger percent biases. For the full period, PBIAS during the summer irrigation period ranged from about 7% to 15%, while during the winter season it ranged from about 9% to 18%, depending on the RCM.

The larger relative differences observed during the winter season should also be interpreted in light of the assumptions adopted for the projected Villoresi Canal discharges. In the scenario construction, winter water availability was included to allow the simulation of different water management practices involving winter discharges. Therefore, winter differences should not be interpreted only as a climate-model effect, but also as the result of assumptions on canal water availability and winter water management.

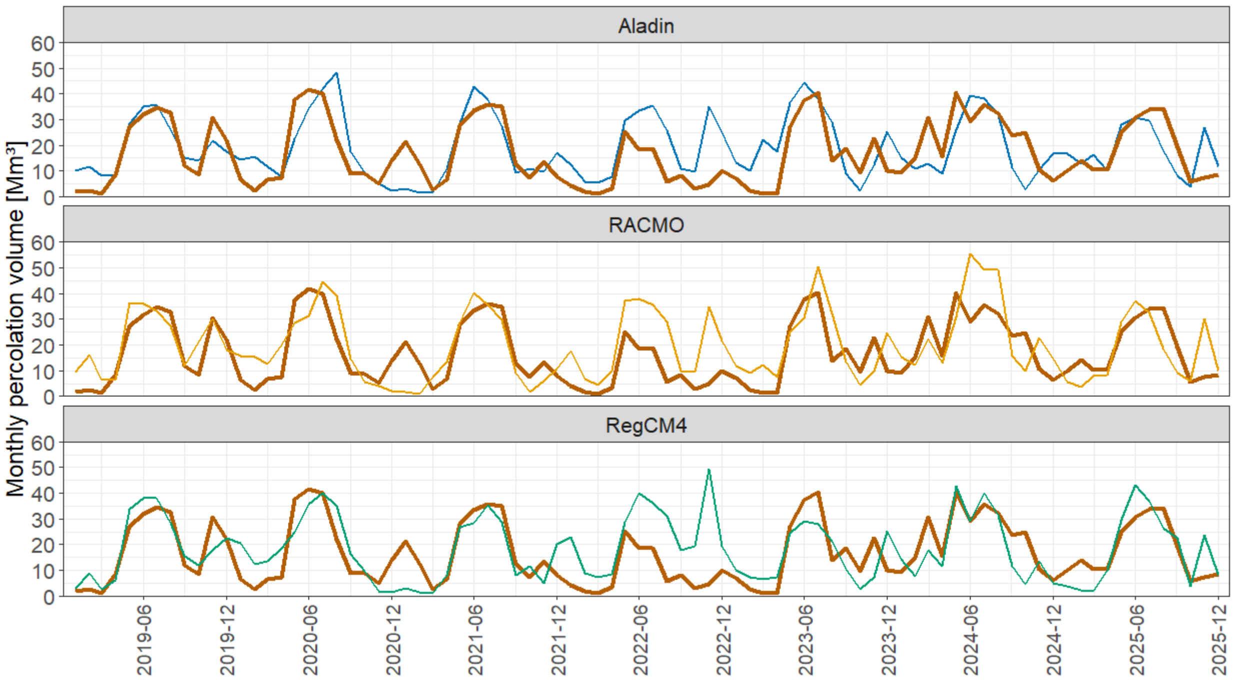

Figure 2. Monthly percolation volume [Mm^3] estimated with the RCM-driven simulations compared to the monthly percolation volume estimated with the historical data for the 2019-25 control period.

To quantify the agreement between RCM-driven simulations and the Historical reference, KGE was selected as a synthetic performance metric because it combines three complementary aspects of the comparison: temporal correlation, variability and mean bias. Its components were also reported to support the interpretation of the results: Pearson correlation (r) describes the agreement in monthly dynamics, alpha indicates whether the variability of the RCM-driven simulation is consistent with the Historical reference, and beta expresses the ratio between simulated and Historical mean percolation and therefore represents the mean bias component. The indices, listed in Table 1, were computed for the full 2019–2025 control period and for a sensitivity case excluding 2022, which was the most anomalous drought year in the reference period.

Table 1. Assessment indices evaluated for the RCM-driven percolation estimates for the entire reference period (2019-25) and excluding 2022.

Period	Scenario	KGE	r	alpha	beta
Full period	Aladin	0.63	0.66	0.97	1.13
Full period	RACMO	0.63	0.69	1.09	1.18
Full period	RegCM4	0.64	0.66	1.03	1.1
Without 2022	Aladin	0.69	0.69	0.97	1.04
Without 2022	RACMO	0.71	0.74	1.1	1.08
Without 2022	RegCM4	0.78	0.78	1	0.96

The monthly performance indices show that, over the full control period, the three RCM-driven simulations have very similar KGE values, ranging between 0.63 and 0.64. This indicates a moderate ability to reproduce the monthly percolation dynamics simulated with historical forcing. The three RCMs reproduce the temporal evolution of monthly percolation reasonably well, as shown by positive Pearson correlation values ranging from 0.66 to 0.69. The variability component is also well represented, with alpha values close to 1 for all simulations. The main discrepancy is related to the bias component: beta is greater than 1 for all RCMs over the full period, indicating a systematic overestimation of mean monthly percolation relative to the Historical simulation.

When 2022 is excluded, the performance improves for all three RCM-driven simulations. KGE increases to 0.69 for Aladin, 0.71 for RACMO and 0.78 for RegCM4, and the correlation also improves. The beta component moves closer to 1, confirming that the extreme drought year strongly affects the comparison with the Historical reference. Aladin and RACMO still show a slight overestimation, whereas RegCM4 shifts to a slight underestimation. Overall, the sensitivity analysis confirms that the lack of representation of the 2022 drought anomaly is a key factor affecting the performance indices, while the RCM-driven simulations better reproduce average monthly conditions when this anomalous year is excluded.

These results provide the basis for interpreting the groundwater simulations and adaptation scenarios presented in the following sections.

C. Groundwater resources under climate change and adaptation scenarios

The climate change scenarios percolation was provided as input to the groundwater model described in D2.3.2 to generate future groundwater levels projections. Then, multiple adaptation scenarios were built adding varying configurations of the tested adaptation measure, as described in Chapter 2. The results of climate change and extreme drought scenarios are presented in Chapters 3 and 4, while the cumulative results of the adaptation scenarios are presented in Chapter 4.

2. Description of the simulated scenarios

2.1. General model configuration

The MODFLOW-USG (Panday et al., 2015) based model utilized for the simulation of projections is based on the calibrated one described in Deliverable 2.3.2. The model was then set to monthly stress periods, from 2023 to 2050. The boundary conditions were left unchanged, aside from extraction wells, recharge and the Villoresi canal. Extractions which were set equal to the average declared discharge in the period 2020-2025. Recharge and Villoresi canal (modeled with SFR) were obtained starting from the projections described in Deliverable 2.4.1. The projected climate data was utilized to obtain the percolation described in Section 1. The projected flow derivation was utilized as the water flow in the Villoresi canal. Further derivations were obtained for the Derivatore di Parabiago based on the historical derivation percentage compared to the circulating volume in the main canal.

2.2. Scenarios description

A total of 192 scenarios were performed. This number is the result of the combination of multiple configurations, listed in Table 2 and explained below.

- **RCM**: three scenarios considering percolation and discharge projections obtained by the downscaling of the regional circulation models (RCM) considered and the derivation modeling described in Deliverable 2.4.1. The regional circulation models utilized are CNRM-ALADIN63, KNMI-RACMO22E and ICTP-RegCM4-6.
- **2022-2023 drought representation**: to assess the effectiveness of the measure under extreme conditions, the 2022-2023 drought was represented cyclically, with a periodicity of seven years, a periodicity observed in historical groundwater time series.
    - Yes: every 7 years from 2025, the conditions of 2022-2023 were reproduced in terms of percolation (obtained through the IdrAgra model) and circulating water in the Villoresi canal, based on observations. The years in which this condition is present are thus 2032-33, 2039-40, 2046-47.
    - No: the climate and discharge projections were not modified.
- **Field distribution**: these configurations reproduce different field distributions in space, to account for the location of lowland springs and their consequent drainage effects. The total discharge provided to the fields was equal to 2.6 m^3/s, equivalent to the average summer discharge on the Derivatore di Bareggio registered from 2000 to 2025 (not considering the extreme years 2022 and 2023). This is an assumption considering the system working at its full capacity, more than what was tested during the

Pilot Action implementation. Another assumption is to consider the totality of this discharge as percolation. In D2.3.2, however, it was observed that less than 3% of distributed water doesn't percolate during the measure. Percolation was assigned both to field cells and canal cells. A coefficient was utilized to obtain the canals losses applying it to the required discharge at the fields. The coefficient was set equal to 0.8 in concrete bedded canals and 0.68 in canals with other conditions, following estimates on the losses described in D2.3.2. The field distribution was decided based on the irrigated fields during summer along Derivatore di Bareggio, the secondary canal utilized in the Pilot Action tests, provided by Consortium Est Ticino Villoresi. To each field was provided an average of 0.09 m^3/s (90 l/s) and the recharge in m/s for each cell was assigned based on the area of the field.

- North: all fields are located North to the lowland spring and CSNO area. Total irrigated area: 326 ha.
- South: all fields are located South to the lowland spring and CSNO area. Total irrigated area: 348 ha.
- Whole area: the fields are distributed across the Derivatore di Bareggio area, independently by the relative location of the fields and lowland springs. Of the total 385 ha area, 76% of the cells are above the CSNO/lowland spring area, equivalent to 64% of the distributed discharge.
- Canals only: in this configuration, the same additional recharge is applied only to cells where a canal was present, along the whole area covered by the Derivatore di Bareggio. This configuration is useful to understand the feasibility of the measure if using only the canal network for the adaptation measure instead of a combination of canals and fields. Of the total 1331 ha area, 67% of the cells and distributed volume are above the CSNO/lowland spring area. The area covered in this configuration is well above the others, this is due to the need to consider each cell crossed by the canals. The result is thus lower intensity discharge (0.002 m^3/s, 2 l/s for each cell) more distributed across the Pilot Area.

- **Implementation strategy**: these configurations define when the adaptation measure is implemented, if it is implemented. For each strategy, the measure is applied in the stress periods corresponding to November, December, January and February, for a total of four months. Combining this information with the discharge provided, a total of 27 Mm^3 gets distributed each winter of implementation.
  - Drought preparedness: the measure is applied in every non-dry year. The dry years are defined as years presenting a cumulative yearly percolation above the median of the whole 2026-2050 period.
  - Drought recovery: the measure is applied in a non-dry year if the previous year is dry. In the scenarios with the 2022-2023 drought representation, the measure is applied only at the end of the 2023 periods (2033, 2040, 2047).
  - Combination of the two: the measure is applied in every non-dry year and at the end of the 2023 periods (2033, 2040, 2047).
  - No implementation: the measure is not implemented.
- **Pumping of water to sustain the extreme drought**: two additional configurations were tested to assess the measure capability of sustaining additional pumping during the extreme drought events. The pumping volume was calculated by obtaining the difference between the average volume distributed in the Derivatore di Bareggio over the 2000-2025 period and the one observed in 2022 and 2023. It was assessed to be equal to 13.5 Mm^3 for 2022 and 4.6 Mm^3 for 2023. This total volume was then considered to be the "missing" volume that, if covered by pumping, could alleviate or compensate the hydrological drought. The volume was divided across five months (April to August, the standard irrigation season in the area) to obtain an average discharge to be extracted: 1.04 m^3/s for 2022 and 0.36 m^3/s for 2023. A total of 29

pumping wells was located upstream to the percolating fields, each extracting the average discharge of existing irrigation wells in the Pilot Area (0.036 m^3/s, or 36 l/s) from April to August. This approach does not consider reductions to the extracted flows resulting from the lower losses of irrigation systems relying on pumping, nor the potential return flow coming from the distribution of the extracted water on the fields. It is thus the most pressing condition.

- Yes, 1 year: the extraction happened only in the summers of the reproduced 2022 conditions (2032, 2039, 2046).
- Yes, 2 years: the extraction happened in the summers of the reproduced 2022 and 2023 conditions (2033, 2040, 2047).
- No: no additional pumping during extreme years.

Table 2. List of the configurations performed. Each model run was obtained by a combination of these configurations, for a total of 216 runs

RCM	2022-2023 drought representation	Field distribution*	Implementation strategy	Pumping of water needed to sustain extreme drought**
CNRM-ALADIN63	Yes	North (no springs)	Drought preparedness	Yes, 1 year
KNMI-RACMO22E	No	South (springs)	Drought recovery	Yes, 2 years
ICTP-RegCM4-6		Whole area (as in field test)	Combination of the two	No
		Only canals	Without implementation	

*Field distribution was not active in the scenarios “Without implementation”
**Pumping is only active in when 2022-2023 drought is represented

3. Groundwater levels and lowland springs variability under climate change and 2022-2023 drougth scenarios

The average groundwater level in the Pilot Area' shallow aquifer under the three climate change scenarios is shown in Figure 3. The three regional circulation models show consistent results in terms of variability and frequency of dry years. All the models project 2040's January being a particularly low water table year, and RACMO simulates two consecutive dry years in 2044-45. These patterns are present also in the lowland springs water flows variability (Figure 4), since the same years showing low water tables also show lower flows.

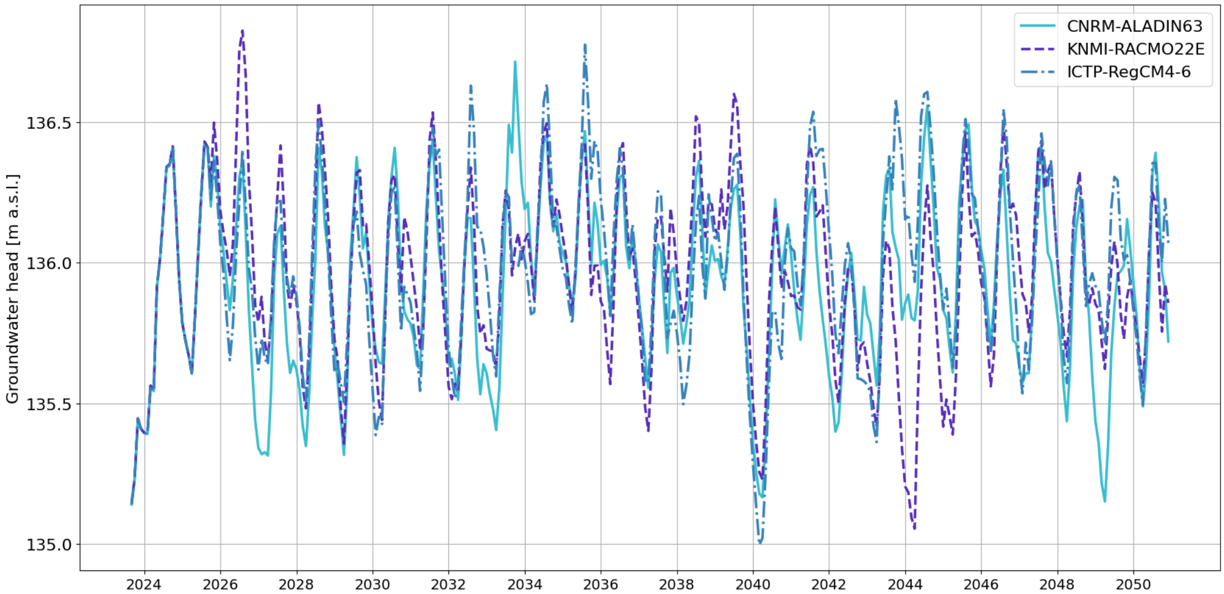

Figure 3. Average groundwater table of the Pilot Area under the three climate change scenarios in terms of percolation and irrigation

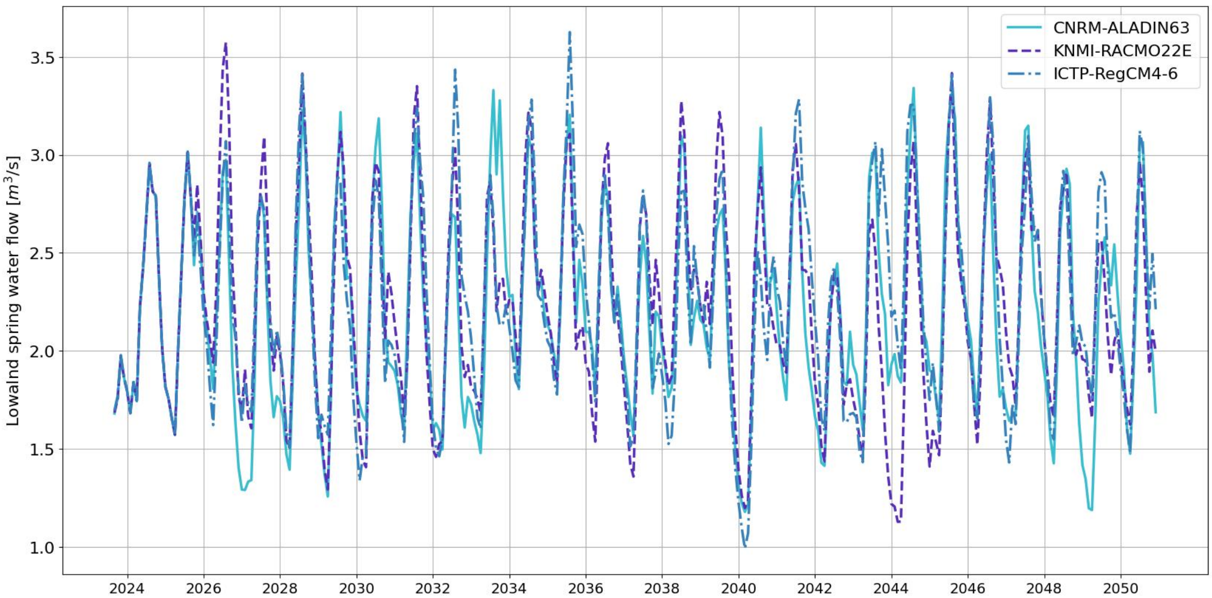

Figure 4. Cumulative lowland spring water flow in the Pilot Area under the three climate change scenarios in terms of percolation and irrigation

Figure 5 shows the groundwater table series simulated considering the 2022-2023 period repeated every seven years. This is an extreme condition, since in the projections no other year was able to reach the low water table obtained at the end of the “2022” (e.g. in April 2033). However, it will be useful in the next section to assess the capabilities of the measure and implementation strategy in recovering and preparing to harsh drought conditions. As observed in the non-modified simulation, lowland springs flows closely follow the water table conditions, thus showing their lowest values during the extreme periods Figure 6.

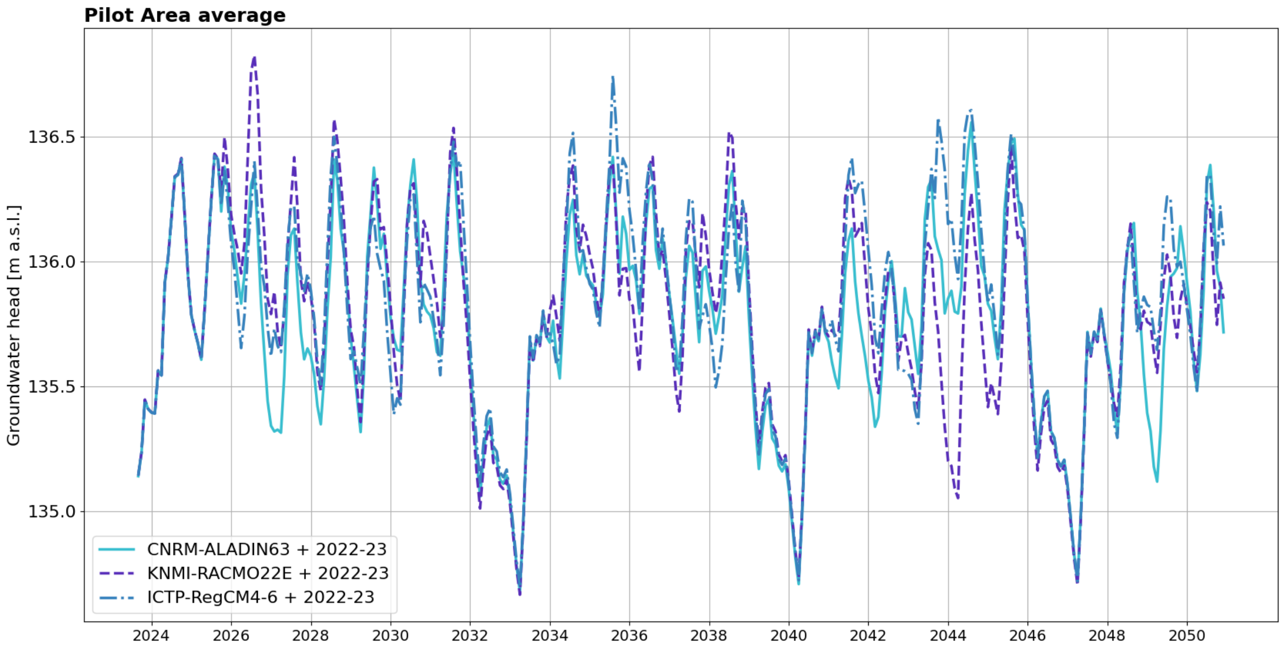

Figure 5. Average groundwater table of the Pilot Area under the three climate change scenarios in terms of percolation and irrigation, introducing 2022-2023 conditions every 7 years

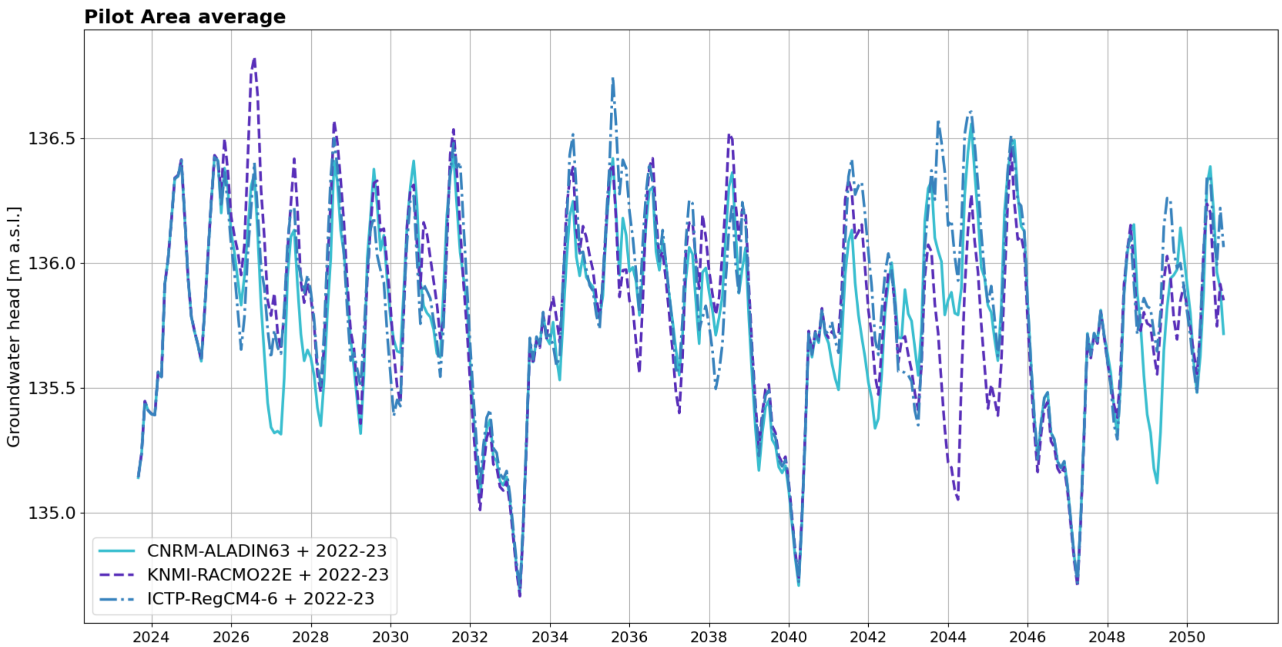

Figure 6. Cumulative lowland spring water flow in the Pilot Area under the three climate change scenarios in terms of percolation and irrigation, introducing 2022-2023 conditions every 7 years

4. Analysis of the proposed agricultural managed aquifer recharge measure reliability in adapting to climate change and extreme periods

4.1. Indicators

4.1.1. Stored volume

One of the goals of the simulations was to understand the efficacy of the measure in storing additional reserves in the aquifer which could then be used in adapting to drought periods. The stored volume at the end of the implementation was obtained as the difference between the groundwater head with and without the implementation multiplied by the effective porosity. In Figure 3, the absolute stored volumes are shown as average across every implementation period in the models. In Figure 8, the percentage of stored volume over the total distributed volume is shown. Considering the total distributed volume (27 Mm^3), the average storage rate at the end of the implementation (1st of March) is equal to 61% (16.4 Mm^3), decreasing to 36% (9.7 Mm^3) at the start of Summer (1st of June). The maximum obtained rate at the end of implementation is 88% (59% at the start of Summer), while the minimum is 30% (12% at the end of the summer). The main reason for this variability is the field distribution, described in detail in Section 4.2. The average result utilizing a similar field distribution to the one tested during the Pilot Action are 65% and 38%. The average storage rate at the end of the implementation is similar among the three RCM utilized, with RegCM4 showing slightly lower storage rates (Aladin: 62.8%, 36.7%; RACMO: 62.8%, 37.1%.; RegCM4: 61.3%, 35.4%).

The implementation strategy influences the volume stored at the end of the implementation. Drought preparedness and Combination strategies show a 7% higher storage than Drought recovery on average. This is due to consecutive years of implementation of the measure. In the Drought preparedness and Combination strategies, on the 25 years of simulation, the measure is implemented in an average of 10 years, of which on average 3 were consecutive years. In the Drought recovery strategy, no consecutive years are present, and the measure is implemented on average in only 4 years. The average volume still stored after one year from the end of the implementation is 2.7 Mm^3, 10%. This volume contributes to the total stored volume by the measure in the next year. This effect is lowered at the start of the summer, coherently with the decrease of the stored volume from the previous year (to 7%). The contribution of the measure decreases under 1% of the total infiltrated volume after 30 months in no consecutive years.

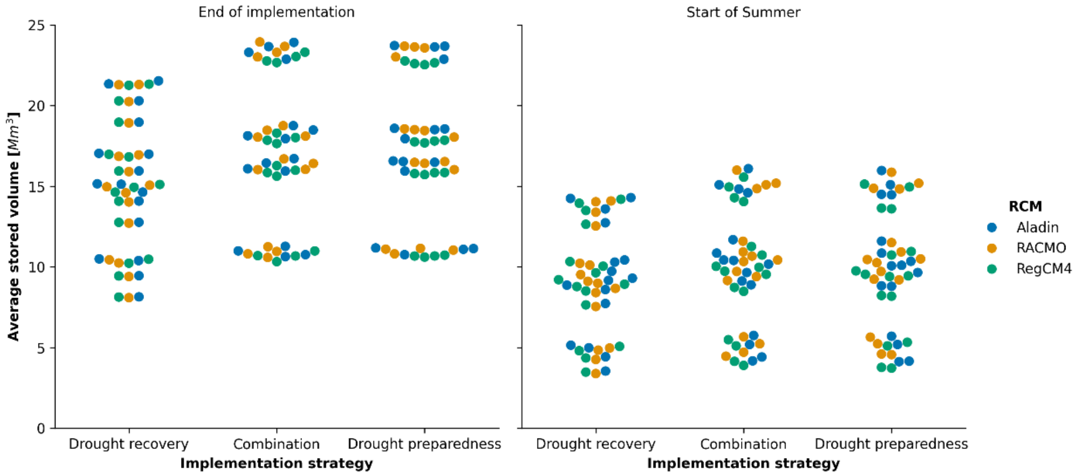

Figure 7. Average total stored volume (Mm^3) at the end of the implementation (1st of March) and at the start of the summer (1st of June) across the whole simulation. Each dot represents a simulation, coloured by the RCM utilized, and the x axis groups them by implementation strategy

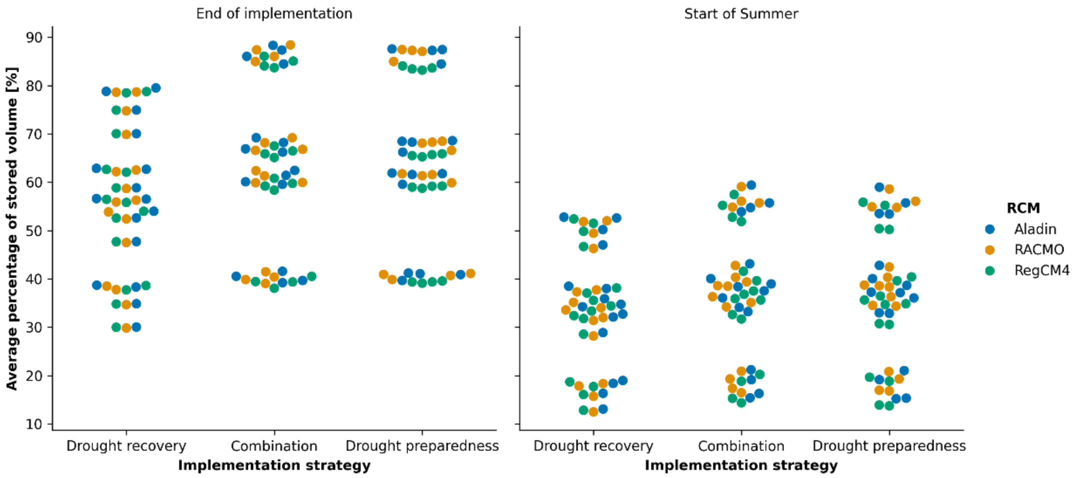

Figure 8. Average percentage of stored volume over the total infiltrated one at the end of the implementation (1st of March) and at the start of the summer (1st of June). Each dot represents a simulation, coloured by the RCM utilized, and the x axis groups them by implementation strategy

4.1.2. Lowland springs

Introduction on lowland springs

Lowland springs are groundwater dependent ecosystems scattered across the whole Pilot Area, for a total of 163. The important notions to understand the following paragraphs and figures are explained here, while a description of them and the results from their monitoring can be found in Deliverable 2.1.1 and 2.1.2. They are depressions in which groundwater meets the surface. Their bed' soil composition can vary from fine sands to loam. Usually, they are composed of a deeper section at their beginning (called head) and a canal shaped section downstream. Groundwater gets primarily drained in the first section and flows them through the canal downstream. This water is usually utilized for irrigation, providing an important source of water for downstream farmers. The presence of water with a relatively stable temperature through the year enabled the flourishing of peculiar and relevant ecosystems. They have encountered a decline in the past decades, mainly due to human influences (Bischetti et al., 2012). Their sustenance is closely linked with the water table level: if the aquifer is high, the springs will activate, if not, they'll remain dry. This is relevant to the outcomes of the Pilot Action: part of the water that gets infiltrated gets drained by these springs. It thus needs to be considered when determining the efficacy of the measure.

In the model, lowland springs are represented through MODFLOW-USG DRN package, meaning that when the water table surpasses the elevation of their bed, water gets drained proportionally to the bed hydraulic conductivity. The average hydraulic conductivity is equal to 3.13 10^{-5} m/s, coherent with the sediments soil composition of silt and fine sand (Bischetti et al., 2012; Gupta et al., 2021). More information on their representation can be found in Deliverable 2.3.2.

Results

Lowland springs react to the implementation of the measure tested in the Pilot Action. The global average of increased discharge is 2.4 l/s per spring. How they react however depends on the measure field distribution, implementation strategy and on the aquifer level. The field distribution effect is evident in Figure 9. At the end of the implementation, the *south* field distribution is the one showing the highest average increase in average lowland springs discharge and in the number of lowland springs increasing more than 10 l/s (Figure 9b) and this is confirmed in springs activating over 2.5 l/s (Figure 9a).*Canals* and *whole* distributions have similar distributions. *North* is the configuration in which the springs get activated less in both cases. At the start of the irrigation period and at the start of the summer the *south* condition is the one showing the sharpest decrease in number of springs and discharge increase. The additional recharge in this configuration is concentrated in the lowland spring area, and more lowland springs gets activated at discharges higher than 10 l/s compared to other configurations. The aquifer gets drained faster, and thus less water remains in the subsequent summer period, while no water is moving from upstream. This results, at the start of summer, in the effect on the lowland springs being reduced by 55% and 80% compared to the end of implementation, considering the number of springs activated and the average discharge, respectively. Broader distributions (*canals, whole*) have a more persisting effect in time considering the number of lowland springs and average discharge (49%, 65% of *canals* and 43%, 65% of *whole*). The *north* distribution shows the most persistent effect on lowland springs, coherently with what was observed on stored volume (see Section 4.2 and Figure 10). This means that although the number of overall lowland springs activated at the end of the implementation is sensibly lower than the other configurations (30 compared to 60), the decrease in terms of average discharge is lower (27%), and the number of active springs stays stable (2% increase). This can be explained from the aquifer dynamics: water infiltrated upstream activates more springs when travelling downstream during the months following the implementation. These considerations are confirmed when considering the conditions in the middle of Summer (1st of July), when the *south* distribution shows the lowest number of springs still benefitting from the measure.

If the goal of the measure is to produce a persistent effect in a high number of lowland springs, the results show that a diffused infiltration measure can result in a reliable compromise between the number of activated spring and the time of activation. A concentrated distribution can instead perform better in one of the two measurements: more springs gets activated if the infiltration is close to them, a more persisting effect is found if the infiltration is further away.

Considering the increase in discharge before and after the implementation period it's possible to understand the influence of the implementation strategy on the lowland springs activation. Figure 5c clearly shows how the drought recovery strategy has a greater effect on the discharge increase (avg. cumulative discharge 2.4 m^3/s) and number of springs activated than the other strategies. This option gets activated after dry periods, when the water table and spring discharge are lower, as seen from the original discharge variation in the models without implementation. What happens is thus a "rebound" effect: the relative conditions are lower, so when the measure is implemented, the same effect becomes more relevant. The contrary happens in the drought preparedness option since it activates in wet conditions, with springs already relatively more active (avg. cumulative discharge -1.6 m^3/s). Coherently, the combined option sits between the other two (avg. cumulative discharge -0.7 m^3/s), skewed towards the drought preparedness one. This becomes particularly evident in the extreme projections. By observing Figure 11 (described in the next section), this does not translate to an increased percentage of water drained by the springs than can reduce the effectiveness of the strategy. The lower stored percentage is due to higher storage obtainable with consecutive years of implementation, as observed in section 4.1.1.

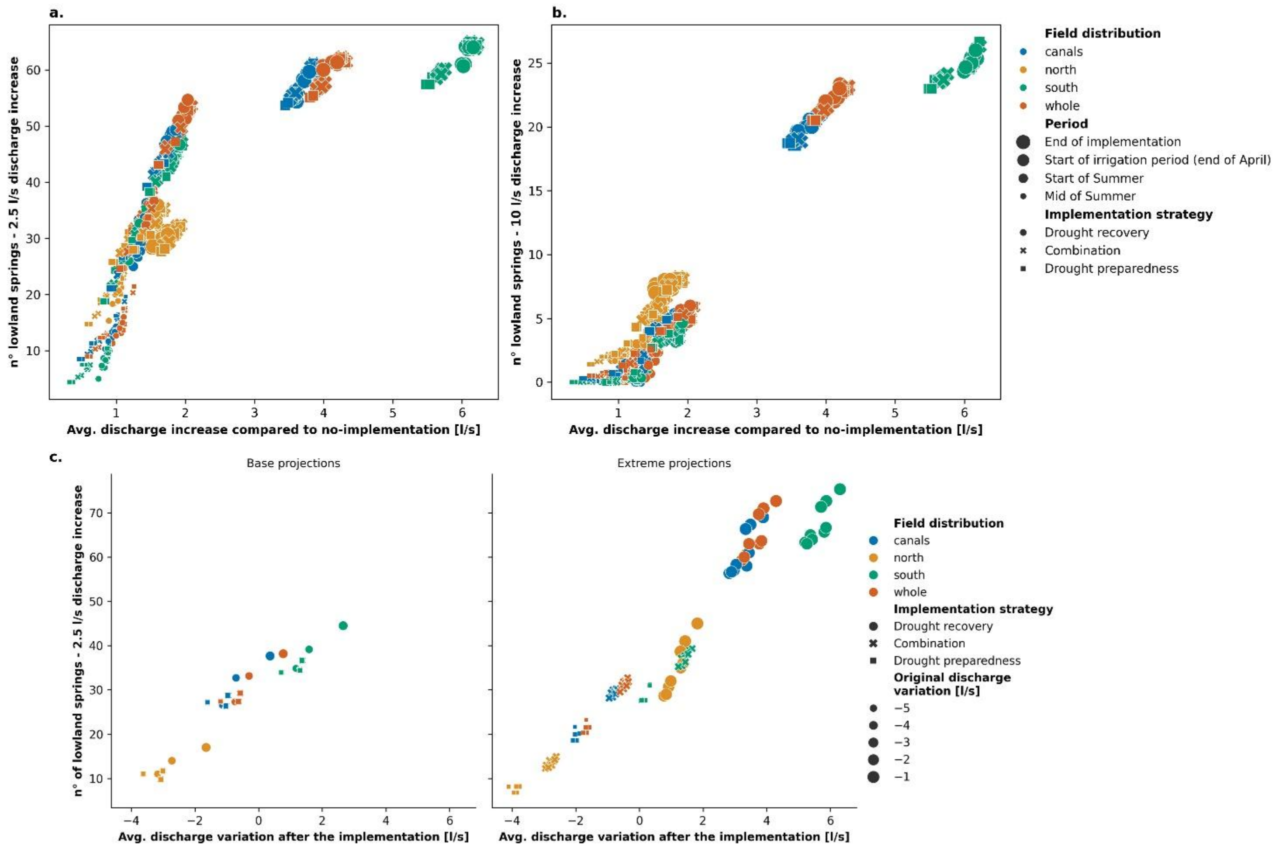

Figure 9. Lowland springs activation due to the implementation of the measure. In a. and b., the differences in discharge and the number of springs with 2.5 and 10 l/s increase are obtained comparing the implementation and no implementation scenarios. In c. the discharge variation is obtained at the end of the implementation comparing it with its initial conditions I the same scenario. The dots size is the average original discharge variation the springs would have had without the implementation

4.2. Impact of field distribution on the stored volume

The effect of field distribution becomes evident distinguishing the scenarios by it, as done in Figure 10 and Figure 11. South, canals, whole and north field distribution scenarios have decreasing areas of infiltration in proximity of lowland springs and of the Canale Scolmatore di Nord Ovest (CSNO). Since they are represented as drains in the model, when the water table increases above their bed elevation, water starts to flow in them. The measure increases the water table more close to the infiltration areas. Higher distance from the infiltration areas thus results in less water getting extracted by them during the implementation and in the following months. The *north* distribution has the highest average percentage of stored volume after the implementation (82%), while the *south* distribution has the lowest (38%). *Whole* and *canals* register 64% and 58%, respectively. The *north* distribution has the most persistency of the stored volume, with a variation from end of implementation to summer equal to -35%, compared to -41%, -41% and -55% in *whole*, *canals* and *south*.

The main reason for this difference is in the percentage of infiltrated water drained by lowland springs and CSNO (Figure 10). In the *south* distribution, 66% on average gets already drained at the end of the implementation, and 78% at the start of summer, compared to 39% and 52% in *canals* and *whole* combined and 17% and 29% in *north*. This effect is due to more lowland springs getting activated in the *south*, *canal* and *whole* field distributions, as observed in Section 4.1.2.

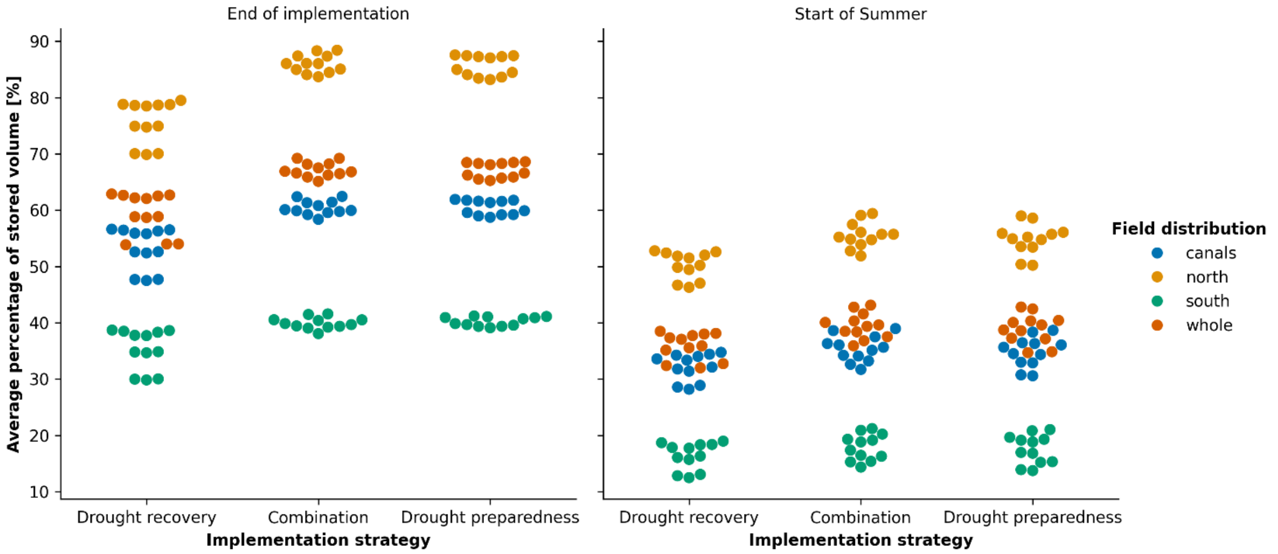

Figure 10. Average percentage of stored volume over the total infiltrated one at the end of the implementation (1st of March) and at the start of the summer (1st of June). Each dot represents a simulation, coloured by the field distribution, and the x axis groups them by implementation strategy

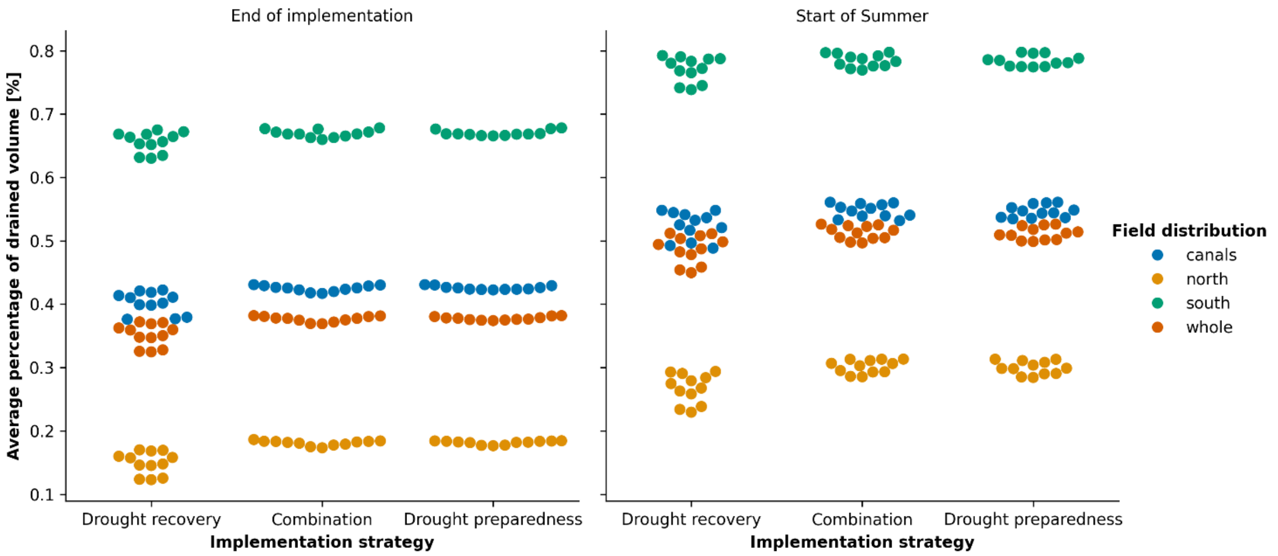

Figure 11. Average percentage of volume drained by lowland springs and CSNO over the total infiltrated one at the end of the implementation (1st of March) and at the start of the summer (1st of June). Each dot represents a simulation, coloured by the field distribution, and the x axis groups them by implementation strategy

North and *south* have been designed specifically to stress the lowland spring behavior, and to obtain two results that could be used as extreme references. They could however raise problems in terms of localized increase of groundwater levels. In Figure 12 is visible how, since they are condensed in dense areas, the induced water level increase in *south* and *north* can reach more than 5 meters close to the infiltration fields. This effect could lead to overflows towards the surface or damages to shallow underground structures, especially in areas where the water depth is low. The maximum induced increase in groundwater levels is lower in the *whole* and *canals* results, having a broader distribution in space. The broader distribution limits the local increase effects, while still enabling storages higher than 60% of the distributed volume at the end of the implementation.

Lowland springs presence thus limits the measure efficacy in storing water in the aquifer, but at the same time limits the groundwater table increase, which may lead to damage. Lowland springs are also very relevant hotspots of biodiversity, which benefit from having a sustained water flow also during the winter. Planning the field location in this measure is thus important to balance the objectives of increased groundwater storage, ecosystem sustenance and groundwater overflow.

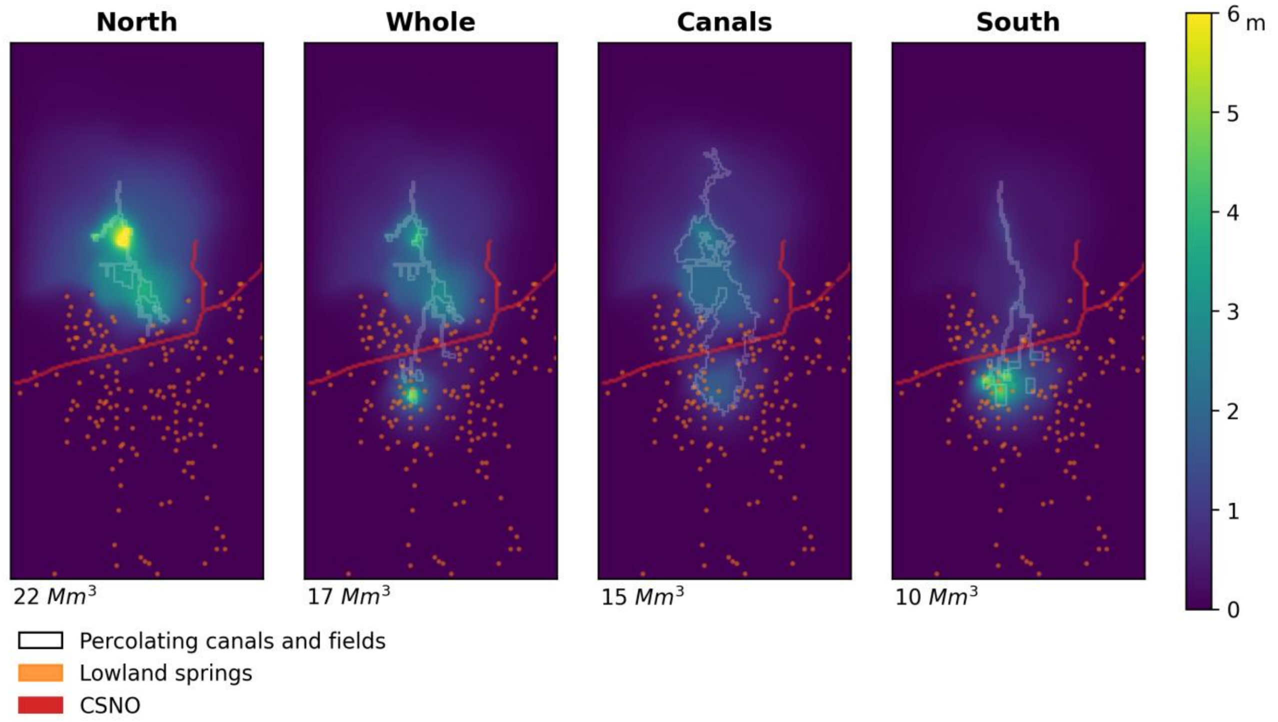

Figure 12. Average groundwater head increase (in meters) at the end of the implementation period across all implementations distinguished by field distribution scenarios. The infiltration fields and canals are shown, as well as the lowland springs and CSNO locations. Below each distribution is reported the average stored volume at the end of the implementation

4.3. Performance in extreme periods

The simulation of the 2022-2023 percolations (2022 was one of driest periods in the history of the Po plain (Montanari et al., 2023)) enabled to consider the performance of the measure under extreme conditions. Scenarios considering an emergency extraction of volume needed to compensate for the drought in the two years were also considered. The results are visualized in Figure 13, averaged over all the tested configurations. With the measure application as a drought recovery option, the aquifer experiences water table levels lower than the non-extreme baseline condition for 32 months, compared to the 42 months without the application. After the end of the extreme period (year 3 in Figure 13a) the measure enables a recovery[1] in 9 months (already in year 3), compared to the 19 needed with no implementation (in year 4), a 24% decrease in the total number of dry months. With no pumping, the decrease is sharper, equal to 39%. In the drought preparedness option (Figure 13b), the effect of the drought condition is alleviated in the first year, with the aquifer being able to sustain it without going into further stress compared to the no-pumping condition. However, the measure is not enough to fully sustain pumping even in the second year. The

[1] The recovery is here considered when difference between the head in the scenario and in the projection is lower than 0.045 m, the average standard deviation of the projection.

combination of the implementation options (Figure 13c) can harness both perks: it is able to sustain the pumping in the first year without stressing the aquifer and it can recover faster after the drought period ended.

The possibility of implementation of the measure after extreme periods is relative to the real availability of water in the tributary river and lake. In autumn and winter 2023, Lake Maggiore and Ticino River conditions were sufficiently good to permit the derivation of 10.5 m^3/s by the Villoresi canal, of which approximately 1.1 m^3/s was utilized in MAURICE experimentations, and would have enabled the 2.6 m^3/s tested in these scenarios. Extractions would still need to be carefully monitored and regulated by authorities and water managers, to avoid stressing the aquifer further than what can be safely recovered.

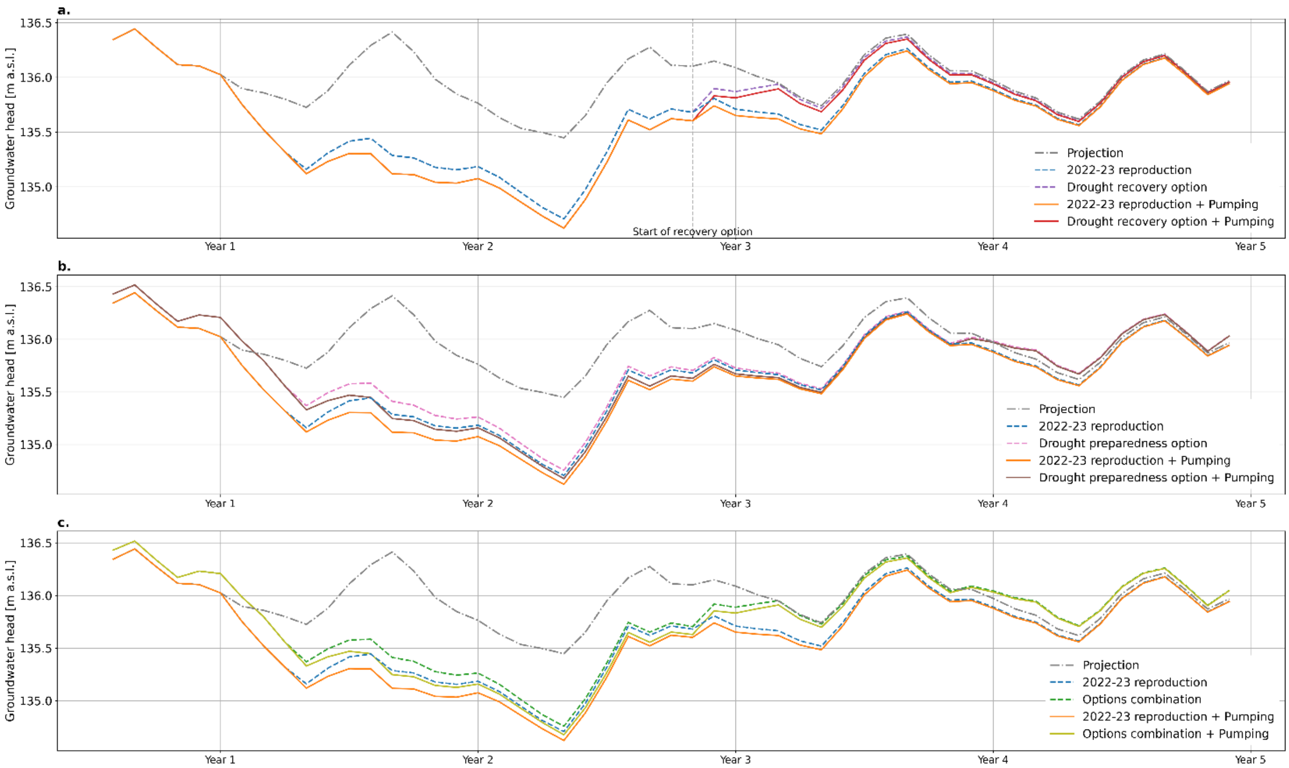

Figure 13. Extreme periods visualization average over the distribution and regional circulation model configurations. The 2 years of emergency pumping scenarios are shown compared to the baseline conditions and extreme simulations without pumping. The subplots a., b. and c. respectively show the results considering the drought recovery, drought preparedness and combination implementation options

D. References

Bischetti, G. B., Fumagalli, N., Piantanida, E. V., Senes, G., Negri, G., Gomarasca, S., Marziali, L., Ferrario, P. S., & Toccolini, A. (2012). *Tutela e valorizzazione dei fontanili del territorio lombardo—FonTe* (No. 144; Quaderni della Ricerca). Regione Lombardia.

Gupta, S., Hengl, T., Lehmann, P., Bonetti, S., & Or, D. (2021). SoilKsatDB: Global database of soil saturated hydraulic conductivity measurements for geoscience applications. *Earth System Science Data*, *13*(4), 1593–1612. https://doi.org/10.5194/essd-13-1593-2021

Montanari, A., Nguyen, H., Rubinetti, S., Ceola, S., Galelli, S., Rubino, A., & Zanchettin, D. (2023). Why the 2022 Po River drought is the worst in the past two centuries. *Science Advances*, *9*(32), eadg8304. https://doi.org/10.1126/sciadv.adg8304

Panday, S., Langevin, C. D., Niswonger, R. G., Ibaraki, M., & Hughes, J. D. (2015). *MODFLOW-USG* [Computer software]. [object Object]. https://doi.org/10.5066/F7R20ZFJ